

## Quantum phase transitions and commensurability in frustrated Josephson junction arrays

C. Bruder, Rosario Fazio, Arno P. Kampf, A. van Otterlo, Gerd Schön

### Angaben zur Veröffentlichung / Publication details:

Bruder, C., Rosario Fazio, Arno P. Kampf, A. van Otterlo, and Gerd Schön. 1992.  
"Quantum phase transitions and commensurability in frustrated Josephson  
junction arrays." *Physica Scripta* 1992 (T42): 159-70.  
<https://doi.org/10.1088/0031-8949/1992/t42/028>.

# Quantum Phase Transitions and Commensurability in Frustrated Josephson Junction Arrays

C. Bruder<sup>a</sup>, Rosario Fazio<sup>b</sup>, Arno Kampf<sup>c</sup>, A. van Otterlo<sup>a</sup> and Gerd Schön<sup>a</sup>

<sup>a</sup> Institut für Theoretische Festkörperphysik, Universität Karlsruhe, 7500 Karlsruhe, FRG

<sup>b</sup> Istituto di Fisica, Università di Catania, viale A. Doria 6, 95128 Catania, Italy

<sup>c</sup> Institut für Festkörperforschung, Forschungszentrum Jülich, 5170 Jülich, FRG

## Abstract

The superconductor-insulator transition of an array of Josephson junctions is studied. In junctions with small capacitance the interaction of charges introduces quantum fluctuations and shifts the phase transition. An external voltage controls the total charge and creates “charge frustration”. Commensurability effects lead to similar structure in the phase diagram as had been found for magnetic frustration. The model used to describe a nonclassical junction array is similar to a Bose-Hubbard model. We study and compare the phase diagrams obtained from both models. If the interaction in the Bose model has a finite range we predict the commensurability to lead to a richly structured dependence on the chemical potential.

## 1. Introduction

Two-dimensional arrays of Josephson junctions have long been studied because of their interesting phase transitions [1]. In classical junction arrays, where the Josephson coupling energy  $E_J$  between neighboring islands is dominant, the configuration of the phases can be characterized by vortices and spin waves. The long range interaction of vortices leads to a Kosterlitz-Thouless-Berezinskii transition [2] where vortex-antivortex pairs dissociate. The transition separates a superconducting low-temperature phase from a resistive high-temperature phase. An applied magnetic field introduces frustration and changes the nature of the phase transition [3].

In junctions with smaller capacitance the interaction of charges gains importance. Charging effects introduce quantum dynamics and, in an array, lower the vortex-unbinding transition temperature. If the charging energy scale  $E_C$  exceeds the Josephson coupling  $E_J$ , there exists no superconducting state even at  $T = 0$  [4]. In most of the theoretical work devoted to this issue the self-capacitance  $C_0$  of the superconducting islands was assumed to dominate over the junction capacitance  $C_1$  [5, 1]. The effect of dissipation due to Ohmic shunt resistors, which allow a continuous flow of charge, or due to quasiparticle tunnelling was also studied [6]. These models were applied to describe the transitions observed in granular films of superconducting material [7].

More recently it became possible to fabricate regular Josephson junction arrays with small capacitances and strong charging effects [8, 9]. In these arrays there are no Ohmic shunts, and the charges change only in discrete quanta due to single electron tunneling or Cooper pair tunneling. Furthermore, the junction capacitances usually dominate over the self-capacitances,  $C_1 \geq C_0$ . Arrays with a general capacitance matrix and discrete charge states have

been studied theoretically [10–16], and the possibility of a charge-ordered, insulating phase was noted [10, 17–22]. The charges and phases of the superconducting islands are quantum mechanical conjugate variables. Charge and vortex order compete and exclude one another. This is most obvious in arrays with  $C_1 \geq C_0$ , where a duality exists between charges and vortices [19–22]. The duality implies a universal conductivity at the superconductor-insulator transition [23]. Similar properties have been observed in superconducting films, which have been described in terms of a Bose-Hubbard model [23, 24].

In the present article we study the effect of frustration on the phase transitions of the quantum phase model and of the Bose-Hubbard model. Magnetic frustration  $f$ , created by a magnetic field, is known to lead to a richly structured, periodic phase diagram. We also investigate charge frustration  $q_x$ , created by an applied voltage which induces a net charge. In the Bose-Hubbard model the equivalent of the charge frustration is the chemical potential  $\mu$ . For short range Coulomb interaction the phase diagram is periodic in  $q_x$  (or  $\mu$ ). For long range interaction the phase diagram shows much more structure, which arises because of the tendency that the ground state charge, configuration is commensurate with the junction lattice. This commensurability property has been overlooked so far, since the Bose-Hubbard model has been studied mostly for on-site Coulomb repulsion only, whereas in the quantum phase model the charge frustration has not been investigated systematically.

In the following Section we introduce the models and a reduced description in terms of charges and vortices, and we comment on the duality between both. In Section 3 we summarize some properties of the phase diagram of arrays without frustration. In Section 4 we derive the phase diagram of the Josephson junction array including the effects of magnetic and charge frustration. The “coarse-graining” approach allows us to analyze this problem in a transparent way. Charge frustration enhances the superconducting phase. The phase diagram consists of lobes of insulating phase, centered around rational values of the charge frustration  $q_x$  (or the chemical potential), separated by superconducting regions. In the lobes, because of the commensurability the total charge (or boson number) remains constant as a function of the charge frustration (or chemical potential), and a correspondingly defined compressibility vanishes. In Section 5 we analyze the conductivity of the array. The insulating state is characterized by a Coulomb gap, which vanishes at the transition. The nature of the

phase transition and the response function differ in the presence or absence of charge frustration. In unfrustrated arrays we recover a universal conductance [23]. It arises since the threshold frequency for the excitation of Josephson plasmon modes vanishes at the transition. In Section 6 we present the analysis of the Bose-Hubbard model, including the effect of amplitude fluctuations. Finally we give a short summary of the main results.

## 2. The models

### The quantum phase model

We consider a regular array of superconducting islands connected by tunnel junctions. In arrays of high quality tunnel junctions there is no flow of Ohmic currents. Hence, the charges can change only in units of  $2e$  due to Cooper pair tunneling or in units of  $e$  due to single electron tunneling. In the present article we further assume that the quasiparticle tunneling is frozen out at the temperatures of interest (for a more general discussion see Refs [18, 19, 22]). Ignoring all fluctuations other than those associated with the phases  $\varphi_i$  of the superconducting order parameters on the islands  $i$  we can describe the system by the Hamiltonian

$$H = \frac{1}{2} \sum_{i,j} (Q_i - Q_{x,i}) C_{ij}^{-1} (Q_j - Q_{x,j}) - \sum_{\langle i,j \rangle} E_J \cos(\varphi_i - \varphi_j - A_{ij}) \quad (1)$$

$$Q_i = \frac{\hbar}{i} \frac{d}{d(\hbar\varphi_i/2e)}.$$

The charge  $Q_i$  on the island  $i$  and the phase  $\varphi_i$  of the islands are quantum mechanical conjugate variables. The Josephson coupling defines the energy scale  $E_J$ . The Coulomb interaction of the charges is described by a capacitance matrix  $C_{ij}$ . For definiteness we consider a square lattice and take into account the self-capacitance of each island  $C_0$  (the capacitance to the ground plane or to infinity), defining an energy scale  $E_0 \equiv e^2/2C_0$ , and the junction capacitance  $C_1$ , defining an energy scale  $E_1 \equiv e^2/2C_1$ , but ignore all other capacitances. Hence  $C_{ii} = C_0 + 4C_1$ ,  $C_{ij} = -C_1$  for  $i$  and  $j$  nearest neighbors, and  $C_{ij} = 0$  otherwise. The charges interact with the inverse capacitance matrix  $C_{ij}^{-1}$ . In the self-charging limit  $C_1 = 0$  this matrix is diagonal. In general the interaction has a finite range, where the ratio of the capacitances determines a screening length  $\Lambda = \sqrt{C_1/C_0}$  (in units of the lattice spacing). In the limit  $C_1 \gg C_0$  the interaction decays logarithmically with distance. For later reference we give  $C_{00}^{-1} \approx (1/4\pi C_1) \ln(16 + 32C_1/C_0)$  and define the quantity  $E_C \equiv e^2 C_{00}^{-1}/2$ . A discussion of more general and realistic models for the capacitances is given in Ref. [18].

Electromagnetic fields are accounted for by a vector potential

$$A_{ij} = \frac{2e}{\hbar c} \int_i^j \mathbf{A} \cdot d\mathbf{l}. \quad (2)$$

In the Hamiltonian (1) we also allowed for "offset" or "external" charges  $Q_{x,i}$  on the islands. They arise for instance due to charged impurities in the substrate, which bind a part of the total island charge. In this case the offset charges are random variables. (In systems with a small number of junctions they can be tuned out by applying suit-

able gate voltages.) We can change the value of the offset charges by applying an overall voltage  $V_x$  between the array and the substrate. In general this introduces a term

$$V_x \sum_i Q_i$$

into the Hamiltonian, where  $\sum_i Q_i$  is the net charge which has traversed the voltage source. Clearly this corresponds to a homogeneous offset charge  $Q_{x,i} = Q_x = C_0 V_x$  in eq. (2). Here we made use of  $\sum_j C_{0j}^{-1} = C^{-1}(\mathbf{k} = 0) = 1/C_0$ .

### The Bose-Hubbard model

Bose-Hubbard models have been studied in various contexts, for instance with the aim to describe the superconductor-insulator transition in thin films [23, 24]. Usually only short range Coulomb interaction between the charged bosons is considered (see, however, [25, 26]). For a more general interaction the Hamiltonian is

$$H = -\frac{1}{2} J \sum_{\langle i,j \rangle} \exp(iA_{ij}) \hat{\Phi}_i^\dagger \hat{\Phi}_j + h.c. + \frac{1}{2} \sum_i V_{ij} \hat{n}_i (\hat{n}_j - \delta_{ij}) - \mu \sum_i \hat{n}_i \quad (3)$$

Here  $\hat{\Phi}_i$  is a Bose annihilation operator,  $\hat{n}_i = \hat{\Phi}_i^\dagger \hat{\Phi}_i$  is the number of bosons at site  $i$ . The total number of bosons is controlled by the chemical potential  $\mu \geq 0$ . The hopping parameter is denoted by  $J$ . Since the bosons are introduced here to represent Cooper pairs of charge  $2e$ , they couple to the vector potential given in (2). We wrote the interaction term such that there is no contribution if a site is occupied with a single boson. We could also account for this by a redefinition of the chemical potential. The similarity of the Bose-Hubbard model and the quantum phase model (1) is obvious; we will compare them further below.

### Charges and vortices

We can describe the Josephson junction array in terms of charges and vortices. In order to do so we express the partition function of the quantum phase model as a path integral in imaginary times  $0 \leq \tau \leq \beta = 1/T$  (from here on we choose  $\hbar = k_B = c = 1$ ). In a mixed representation involving the phases  $\varphi_i(\tau)$  and charge trajectories  $q_i(\tau) \equiv Q_i(\tau)/2e = 0, \pm 1, \pm 2, \dots$  the partition function is

$$Z = \prod_i \int_{q_{i0}}^{q_{i\beta}} \mathcal{D}q_i(\tau) \sum_{\{n_i\}} \exp\left(i2\pi \sum_i q_{x,i} n_i\right) \times \prod_i \int d\varphi_{i0} \int_{\varphi_{i0}}^{\varphi_{i\beta} + 2\pi n_i} \mathcal{D}\varphi_i(\tau) \exp\{-S[q, \varphi]\}. \quad (4)$$

It depends on the action,

$$S[q, \varphi] = \int_0^\beta d\tau \left[ 2e^2 \sum_{i,j} (q_i - q_{x,i}) C_{ij}^{-1} (q_j - q_{x,j}) - \sum_{\langle i,j \rangle} E_J \cos(\varphi_i - \varphi_j - A_{ij}) \right]. \quad (5)$$

In the absence of Ohmic shunts or other continuous flows of charge we are allowed to restrict ourselves to discrete charge states ( $Q_{x,i}$  plus integer multiples of  $2e$ ) only. This implies that values of the phase which differ by  $2\pi$  are equivalent, and the integral in (4) includes a summation over winding

numbers  $\varphi_i(\beta) = \varphi_i(0) + 2\pi n_i$  and a  $Q_x$ -dependent phase factor [27].

The Villain transformation, which can be generalized to the present problem with charges [19, 28], allows us to integrate out the phases at the expense of introducing at each (dual) space-time lattice point an integer-valued field  $v_i(\tau) = 0, \pm 1, \dots$ , the vorticity in the plaquette  $i$ . As a result the partition function can be written as a sum over integer valued paths  $q_i(\tau)$  and  $v_i(\tau)$

$$Z = \sum_{\{q_i(\tau)\}} \sum_{\{v_i(\tau)\}} \exp \{-S[q, v]\}. \quad (6)$$

The action in the charge-vortex representation is

$$S[q, v] = \int_0^\beta d\tau \sum_{i,j} \left[ 2e^2(q_i - q_{x,i})C_{ij}^{-1}(q_j - q_{x,j}) + \frac{1}{4\pi E_j} \dot{q}_i G_{ij} \dot{q}_j + \pi E_j(v_i + f_i) \times G_{ij}(v_j + f_j) - iq_i \Theta_{ij} \dot{v}_j \right]. \quad (7)$$

Here we introduced the frustration  $f_i$  which is the magnetic flux through the plaquette  $i$ , measured in units of the flux quantum  $\Phi_0 = hc/2e$ . For transparency we consider here only static external fields (see Ref. [22] for a more general discussion). The kernel  $G_{ij} = G(\mathbf{r}_i - \mathbf{r}_j)$  describes the interaction between vortices

$$G(\mathbf{r}) = \frac{1}{2\pi} \int d^2q \frac{1}{q^2} [\exp(i\mathbf{q} \cdot \mathbf{r}) - 1] \approx -\frac{1}{2} \ln(2\pi r), \quad (8)$$

which for large distances depends logarithmically on  $r$ . The kernel

$$\Theta_{ij} = \arctan \left( \frac{y_i - y_j}{x_i - x_j} \right), \quad (9)$$

where  $\mathbf{r}_i = (x_i, y_i)$ , describes the phase configuration at site  $i$  around a vortex at site  $j$ . The first and third term in (7) represent the classical action of the electric charges and of the vortices. The interaction between the two types of excitations is described by the fourth term. Obviously this is the interaction energy of a charge  $q_i$  with the voltage  $\Theta_{ij} \dot{v}_j$  at site  $i$ , which is created by the changing vorticity at site  $j$ .

The action (7) shows a high degree of symmetry between the vortex and the charge degrees of freedom. In the limit  $C_1 \gg C_0$  the inverse capacitance matrix becomes (for large distances)

$$e^2(C_{ij}^{-1} - C_{00}^{-1}) = \frac{E_1}{\pi} G_{ij} \quad \text{where} \quad E_1 = e^2/2C_1. \quad (10)$$

In this case charges and vortices are (nearly) dual. The duality is broken by the term  $\dot{q}_i G_{ij} \dot{q}_j$ . It arises as the spin-wave contribution to the charge correlation function. An equivalent term involving  $\dot{v}_i$  does not arise, since in the charge gas defined by the model (2) the corresponding excitations are absent.

### 3. Phase transitions in unfrustrated junction arrays

We briefly discuss the phase transitions in a junction array without external fields and off-set charges,  $\mathcal{A} = 0$  and  $Q_x = 0$ . For a more extensive discussion we refer to Refs [19, 22]. In classical junctions with large capacitance  $E_c \ll E_j$  the

action (7) reduces to the Hamiltonian of the classical Coulomb gas of vortices. The system has a Kosterlitz-Thouless-Berezinskii (KTB) transition, where vortex dipoles unbind, at a temperature  $T_v^{(0)} = (\pi/2)E_j$ . (We ignored a dielectric constant which is close to one.) This transition separates a superconducting from a resistive phase. If  $E_j = 0$  the problem reduces to the classical Coulomb gas of charges. If the junction capacitance dominates  $C_1 \gg C_0$  the charges interact logarithmically over sufficiently long distances; and also this system has a KTB transition. But now charge dipoles, formed by a Cooper pair and a missing pair, unbind. The transition temperature is  $T_c^{(0)} = E_1/\pi$ . It separates an insulating from a conducting phase.

At finite  $E_j$  and  $E_c$  both charges and vortices need to be considered simultaneously. The charging energy provides a kinetic energy for the vortices, vice versa the Josephson coupling allows the tunneling of Cooper pairs and provides the dynamics for the charges. If the charging energy  $E_0$  or  $E_1$  is still small compared to  $E_j$  we can show in a perturbative approach that the transition temperature of the vortex-unbinding KTB transition is lowered below the classical value  $T_v^{(0)}$ . Similarly, in the limit  $C_1 \gg C_0$  weak Cooper pair tunneling  $E_j \ll E_1$  lowers the charge unbinding transition temperature below  $T_c^{(0)}$  [19]. Further conclusions depend not only on the ratio of Josephson coupling energy and charging energy, but also on the form of the capacitance matrix. Let us first consider the limit where the junction capacitance dominates.

#### Arrays with charge-vortex duality

In the limit  $C_1 \gg C_0$  the duality between charges and vortices allows us to draw further conclusions. If the duality were perfect (i.e. if the duality breaking last term in (7) were absent) the transition temperatures would be symmetric around the self-dual point

$$(E_j/E_1)_{\text{self-dual}} = 2/\pi^2. \quad (11)$$

By independent arguments we had shown [19] that at  $T = 0$  there exists only one transition. From this we can immediately conclude that at  $T = 0$  there exists an insulator-superconductor transition, separating a charge- from a vortex-ordered phase, and the critical value of  $E_j/E_1$  is given by (11). The duality breaking term, even if it becomes irrelevant at the fixed point, shifts the critical point to a value which exceeds (11) by a factor of order one. Combining this information with the perturbative results (but ignoring the shift due to the lack of perfect duality) we arrive at the picture shown qualitatively in Fig. 1.

The duality also allows us to draw conclusions about the response of the system. The charges are driven by an applied voltage, and their motion produces a current. On the other hand, the vortices are driven by an applied current, and their motion produces a voltage. The duality between charges and vortices at the superconductor-insulator transition implies that the resistance of the array exactly at the transition is given by the quantum resistance  $R_q = h/4e^2 = 6.45k\Omega$  [23]. We will comment further on this result in Section 5 where we evaluate the conductivity of the system near the transition.

#### General capacitance matrix

If  $C_1$  is not much larger than  $C_0$  the interaction of the charges is screened. Since the requirements for an insulating,

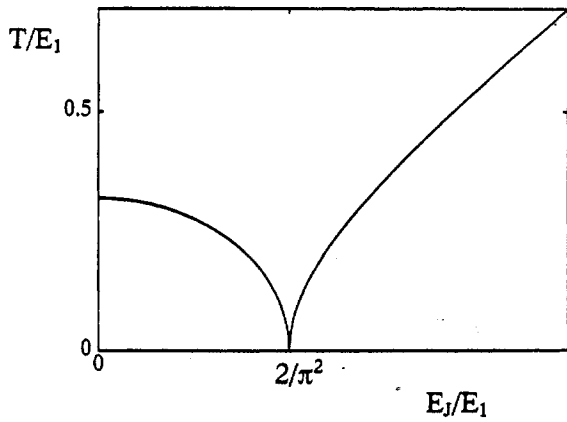


Fig. 1. Transition temperatures as a function of  $E_J/E_1$  for the vortex unbinding transition (large  $E_J/E_1$ ) and the charge unbinding transition (small  $E_J/E_1$ ) in a junction array with  $C_1 \gg C_0$ .

charge ordered phase are not satisfied the phase diagram looks simpler. Results will be shown below. There exist only two phases, a low temperature superconducting phase at sufficiently large values of  $E_J/E_C$ , and a disordered phase at higher temperatures, which extends down to  $T = 0$  for small values of  $E_J/E_C$  [5]. The nature of the disordered phase deserves a comment. Since our model does not include an explicit mechanism for dissipation, the system can only have an infinite or a zero dc-conductivity [29]. However, at finite temperatures, in the presence of dissipation, or at finite frequencies the disordered phase in general is resistive. This differs from the case where the charges interact logarithmically over long distances, where the insulating phase exists also at finite temperatures and in the presence of dissipation. Detailed studies of dissipative junction arrays have revealed that the  $T = 0$  phase diagram shows more distinct phases, depending on the strength of the dissipation and the Josephson coupling [30, 31]. The phases differ in their correlation functions in space and time direction and have different response functions. Another question has remained controversial in the literature, namely whether or not the phase diagram is reentrant [5, 6]. Below we will show, within our approximation scheme, that the answer depends on the allowed charge states.

#### 4. Phase transitions in junction arrays with frustration

The properties of junction arrays and their phase transitions are influenced by both external magnetic fields and external charges. In the classical case the influence of the magnetic field has been studied extensively, and a complicated periodic dependence on  $f$ , the flux per unit cell in units of the flux quantum, has been found [1, 3]. This arises because of commensurability between the vortex lattice and the underlying junction array. In the quantum case the phase diagram depends in a nontrivial way on  $f$  as well. This has been demonstrated for a system with Ohmic dissipation, and hence a continuum of charges, in Ref. [32]. In disordered lattices the commensurability plays no role, but the magnetic field can still lead to a "field tuned transition". Several scaling predictions of the theory [33] have been verified in disordered films [34]. Recently a transition with similar scaling properties has been observed in regular, fabricated junction arrays with suitable parameters [35]. It occurs at values of  $f$  close to an integer, together with the expected flux periodicity. However, the picture is more complex than

in disordered films. For instance, another transition occurs near  $f = 1/2, 3/2, \dots$  (see also [36]).

#### The coarse-graining approximation

In order to study the system with frustration we make use of the so-called "coarse graining" approximation developed by Doniach [37]. The essence of this approach is to introduce a complex order parameter field  $\psi$ , whose expectation values is proportional to that of  $\exp(i\phi)$ . As long as  $\psi$  is small, i.e. close to the onset of phase coherence, the system is governed by an effective Ginzburg-Landau functional. The method has been discussed in the literature, but we briefly recapitulate it.

By introducing  $\xi_i(\tau) = \exp[i\phi_i(\tau)]$  and a Hubbard-Stratonovich field  $\psi_i(\tau)$ , we can write the Josephson term as

$$-E_J \sum_{\langle i, j \rangle} \cos(\phi_i - \phi_j - A_{ij}) = -\frac{E_J}{2} \sum_{\langle i, j \rangle} \gamma_{ij} e^{iA_{ij}} \xi_i^*(\tau) \xi_j(\tau) \quad (12)$$

where  $\gamma_{ij} = 1$  for nearest neighbors and zero otherwise. The partition function becomes

$$Z = \int \prod_i \mathcal{D}\psi_i(\tau) \exp\{-F[\psi]\} \quad (13)$$

with the Ginzburg-Landau functional

$$F[\psi] = \int_0^\beta d\tau \sum_{ij} \psi_i^*(\tau) \frac{2}{E_J} \gamma_{ij}^{-1} \psi_j(\tau) \exp(-iA_{ij}) - \log \left\langle \exp \left\{ - \int_0^\beta d\tau \sum_i [\xi_i(\tau) \psi_i^*(\tau) + c.c.] \right\} \right\rangle_0 \quad (14)$$

Here and in the following,  $\langle \dots \rangle_0$  refers to expectation values computed with the charging energy  $S_0$

$$S_0 = \int_0^\beta d\tau \frac{1}{2} \sum_{ij} \frac{\phi_i(\tau)}{2e} C_{ij} \frac{\phi_j(\tau)}{2e} \quad (15)$$

and including the effect of offset charges. Since in our model the charges change only in discrete quanta of  $2e$  the path integrals include a summation over winding numbers and the phase factors  $\exp(2\pi i n_i q_{x,i})$  as shown in eq. (4). This has interesting consequences; for instance the correlation functions in general differ for continuous and discrete charges. (An example is presented in the Appendix.)

Performing a cumulant expansion we obtain to second order in  $\psi$

$$F[\psi] = T \sum_{\mu} \sum_{ij} \left[ \frac{2}{E_J} \gamma_{ij}^{-1} e^{-iA_{ij}} - g_{ij}(\omega_{\mu}) \right] \psi_i^*(\omega_{\mu}) \psi_j(\omega_{\mu}) \quad (16)$$

which depends on the correlation function

$$g_{ij}(\tau) = \langle \exp \{ i[\phi_i(\tau) - \phi_j(0)] \} \rangle_0 = \delta_{ij} g(\tau) \quad (17)$$

A virtue of the coarse-graining approach is the simple structure of (16). All the dependence on the offset charges is contained in the correlation function  $g(\omega_{\mu})$ , while all the magnetic field dependence is still explicit in the first term. Since the charging energy depends on  $\phi_j$  only, the correlation function  $g_{ij}$  is diagonal in the site index even for non-diagonal capacitance matrices. In the following we will consider the effect of a homogeneous magnetic field  $f_i = f$  and of an external voltage, which is described by a homogeneous offset charge  $q_{x,i} = q_x$ . This means that we can suppress the site-index in  $g_{ii} = g$ .

### Charge-frustration

If no magnetic field is applied  $f = 0$ , we can rewrite (16) in a Fourier representation

$$F[\psi] \approx T \sum_{k, \mu} \left[ \varepsilon + \frac{k^2}{8E_C g(0)} + i\omega_\mu \lambda + \zeta \omega_\mu^2 \right] |\psi_k(\omega_\mu)|^2. \quad (18)$$

Here we have absorbed a factor of  $\sqrt{E_C g(\omega_\mu)/E_J}$  in  $\psi_k(\omega_\mu)$ , where  $E_C = e^2 C_{00}^{-1}/2$ . We also expanded  $\gamma^{-1}(k)$  and  $g(\omega_\mu)$  to second order in  $k$  and  $\omega_\mu$ , with the result

$$\varepsilon(T, E_J, C^{-1}, q_x) = \frac{1}{2E_C g(\omega_\mu = 0)} - \frac{E_J}{E_C}$$

$$\lambda = - \frac{1}{2E_C g^2} \left. \frac{dg(\omega_\mu)}{d\omega_\mu} \right|_{\omega_\mu=0}$$

$$\zeta = \frac{1}{4E_C g^2} \left. \frac{d^2 g(\omega_\mu)}{d\omega_\mu^2} \right|_{\omega_\mu=0} - 2E_C g \lambda^2. \quad (19)$$

The mean-field phase boundary is given simply by the condition

$$\varepsilon(T, E_J, C^{-1}, q_x) = 0. \quad (20)$$

Next we have to determine  $g$ . In the homogeneous problem considered here, without loss of generality, we concentrate on the correlation function at the site  $i = 0$ . At low temperatures it is favorable to evaluate it in the charge representation [10]. If we start from the phase representation (15) of  $S_0$  we obtain the charge representation by performing a Poisson resummation. The result (for homogeneous values of  $q_x$ ) is

$$g(\omega_\mu = 0) = \frac{1}{Z_0} \frac{1}{2E_C} \sum_{(q_i)} \frac{\exp \left[ -2e^2 \beta \sum_{ij} (q_i - q_x) C_{ij}^{-1} (q_j - q_x) \right]}{1 - 4 \left[ \sum_j C_{0j}^{-1} (q_j - q_x) / C_{00}^{-1} \right]^2}$$

$$Z_0 = \sum_{(q_i)} \exp \left[ -2e^2 \beta \sum_{ij} (q_i - q_x) C_{ij}^{-1} (q_j - q_x) \right] \quad (21)$$

The sums run over all integer charge configurations on each site. The derivation is sketched in the Appendix.

*Self-charging limit.* In the self-charging case  $C_{ij}^{-1} = \delta_{ij}/C_0$  both the numerator and the denominator  $Z_0$  of the expression (21) factorize into terms which depend on the charge of one island only. Hence,

$$g(\omega_\mu = 0) = \frac{1}{Z_{00}} \frac{1}{2E_0} \sum_q \frac{\exp [-4\beta E_0 (q - q_x)^2]}{1 - 4(q - q_x)^2}. \quad (22)$$

(The expression for  $Z_{00}$  is obvious). At low temperatures the sum is dominated by that integer-valued charge  $q$  which makes the exponent smallest. For  $-\frac{1}{2} \leq q_x \leq \frac{1}{2}$  this value is  $q = 0$ , and the result is simply

$$g(\omega_\mu = 0) = \frac{1}{2E_0} \frac{1}{1 - 4q_x^2}$$

At  $q_x = \frac{1}{2}, \frac{3}{2}, \dots$  the dominant value of  $q$  jumps to 1, 2, ... which makes  $g(\omega_\mu = 0)$  a periodic function.

In Fig. 2 we show the phase boundary (for the self-charging limit  $C_0 \gg C_1$ ) between the disordered (insulating or resistive) and the superconducting phase for different temperatures as a function of  $q_x$ . At low temperatures we find pronounced lobes periodic in  $q_x$  of insulating phase

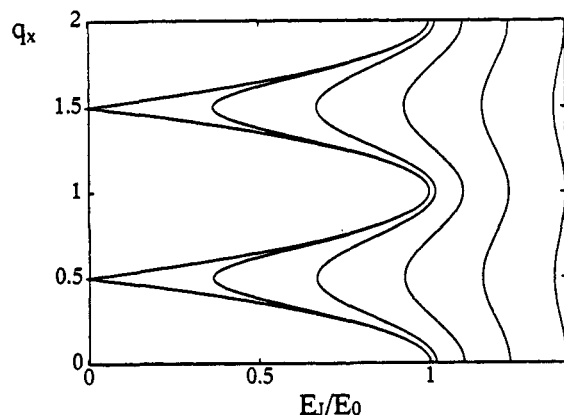


Fig. 2. Phase boundary between the disordered phase (left side) and the superconducting phase (right side) of an array in the self-charging limit  $C_0 \gg C_1$  for temperatures between (from left to right)  $T/E_0 = 0$  and  $T/E_0 = 2$  in intervals of 0.4, as a function of  $q_x$ . Finite  $q_x$  favors superconductivity since it will frustrate the charge order, and for  $q_x = \frac{1}{2}$  and  $T = 0$  the superconducting phase is seen to exist for arbitrarily small values of  $E_J/E_0$ .

separated by regions of superconducting phase. These were known already from the analysis of the Bose-Hubbard models [23, 24]. Finite  $q_x$  frustrates the charge order and favors superconductivity. For  $q_x = \frac{1}{2}$  and  $T = 0$  the superconducting phase exists for arbitrarily small values of  $E_J/E_0$ .

In the insulating lobes the expectation value of the charge per island is integer, forming plateaus when viewed as a function of  $q_x$ . The analysis presented here allows us to draw this conclusion only for infinitesimal values of  $E_J$ . However, it is reasonable to assume that this property does not change as long as we stay away from the phase transition. It is also supported by the results of the quantum Monte Carlo studies of Refs [24, 38, 40]. The transition between the plateaus occurs in the superconducting phases separating the lobes. For small  $E_J$  this transition occurs in a narrow range of  $q_x$  near half-integer values, for larger  $E_J$  the transition region becomes broader. However, the transition is always from one integer value to the next one. This is a consequence of the factorization of the correlation function  $g(\omega_\mu = 0)$  in the self-charging limit. As a result in the ground state each island has the same value of the charge, which changes at the same value of  $q_x$ . For a general capacitance matrix considered below we will find a more complex behavior.

Since charge fluctuations are suppressed exponentially at low  $T$  their effect is weak, and the critical value of  $(E_J/E_0)_{cr}$  depends only weakly on  $T$  [10]

$$\left( \frac{E_J}{E_0} \right)_{cr} = 1 + \frac{8}{3} e^{-4E_0/T}$$

This can be clearly seen in Fig. 3 where we plot the phase boundary as a function of temperature.

If we allow the charges to take all continuous values, for instance because of a continuous flow of currents the presence of Ohmic shunts, the correlation function is given by the function  $g_c$  presented in the Appendix. In this case the phase diagram obtained with the coarse-graining approach (but also in several other approximations) is reentrant. This means there exists a range of values of  $E_J/E_0$  where with increasing temperature the system moves from a disordered phase into the superconducting phase and back into the disordered phase. In contrast, when the charges can take only

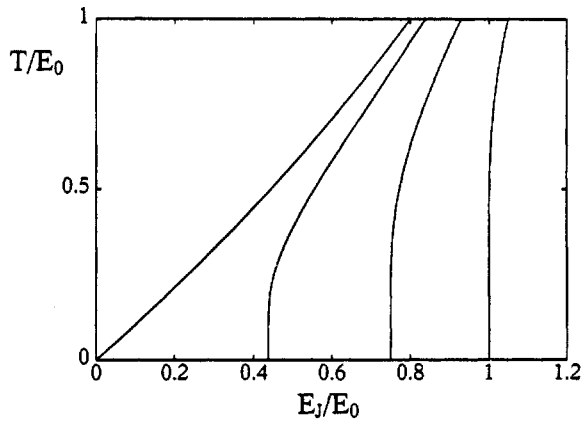


Fig. 3. Phase boundary in the self-charging limit  $C_0 \gg C_1$  between the disordered phase (left side) and the superconducting phase (right side) as a function of temperature for  $q_x = 0, \frac{1}{4}, \frac{3}{8}$  and  $\frac{1}{2}$  (from right to left). For the problem considered here, where the charges take only discrete values, there is no reentrant behavior in contrast to the case of continuous charges

discrete values, which is what we consider here, the phase diagram shows no reentrant behavior.

For the discussion of the response of the system we have to determine also the other coefficients in the GL free energy (18). They are periodic in  $q_x$ . The coefficient  $\lambda$  is an odd function of  $q_x = 0$ , whereas  $\zeta$  is even. In the self-charging limit for  $T = 0$  they can be evaluated explicitly. For  $-\frac{1}{2} \leq q_x \leq \frac{1}{2}$  they are

$$\begin{aligned} \lambda &= q_x/E_0 \\ \zeta &= 1/16E_0^2 \end{aligned} \quad (23)$$

A nonzero value of  $\lambda$  for  $q_x \neq 0$  leads to the appearance of a first order time derivative (with respect to the imaginary time  $\tau$ ) in the Ginzburg-Landau functional. This term should not be interpreted as a dissipative term. It is obtained in other field-theoretical treatments of Bose systems as well (see e.g. [41] and Section 6 of the present work). It obviously depends on excess charges and, for instance, gives rise to a Magnus force on vortices [41, 22]. A dissipative term (e.g. Ohmic dissipation) is described by a term involving  $|\omega_\mu|$  [42].

*General capacitance, finite range of the Coulomb interaction.* For a general capacitance matrix the correlation function does not factorize and is more complicated to evaluate. At low temperatures the sum in (22) is still dominated by the charge configuration which minimizes the charging energy. The total energy can be written as

$$E(\{q_j\}, q_x) = 2e^2 \sum_{i,j} q_i C_{ij}^{-1} q_j - 4 \frac{e^2}{C_0} q_x q_\Sigma + 2N \frac{e^2}{C_0} q_x^2. \quad (24)$$

Here we introduced the total charge  $q_\Sigma = \sum_j q_j$  and made use of the relation  $\sum_j C_{0j}^{-1} = C^{-1}(\mathbf{k} = 0) = 1/C_0$ . The solution of the problem reduces to the following steps:

(i) For a given total charge  $q_\Sigma$  we have to find the configurations of the  $\{q_i\}$  which minimize the first term in the energy (24). (This is a nontrivial problem because of commensurability and degeneracy. The problem is similar to finding the minimum energy configuration of vortices in a Josephson array with frustration, examples of which are discussed in Refs [3].

(ii) For a given  $q_x$  we have to find the value of the total charge  $q_\Sigma$  which yields the lowest energy.

(iii) After having determined the configuration with minimum energy we evaluate the correlation function (21) and determine the mean field phase boundary.

Results for a finite system with periodic boundary conditions are shown in Fig. 4. The commensurability of charge distribution and underlying lattice provides a richly structured phase diagram with many lobes centered around rational values of  $q_x$ . The result shown refers to a small system, but at least some of the lobes keep a finite width in the infinite system limit. For instance the width of the lowest lobe around  $q_x = 0$  for  $E_j = 0$  is given by  $\Delta q_x = C_0 C_{00}^{-1} \approx (C_0/4\pi C_1) \ln(16 + 32C_1/C_0)$ . At  $q_x = 0$  it extends to  $E_j/E_C = 1$ . Also the lobe around  $q_x = \frac{1}{2}$  maintains a finite width  $\Delta q_x = C_0 C_{00}^{-1} - 1/(1 + 8C_1/C_0)$ , and at  $q_x = \frac{1}{2}$  it extends to  $E_j/E_C = 1 - 1/[C_{00}^{-1}(C_0 + 8C_1)]^2$ . In the self-charging limit we have only one big lobe around integer values of  $q_x$ . In the opposite limit  $C_1 \gg C_0$  all lobes have widths which vanish with increasing system size.

If we increase  $q_x$  (say, from 0 to 1) we find that a sequence of inhomogeneous charge configurations made up of  $q_j = 0, 1$  minimizes the charging energy. The average value of  $q_j$ , i.e.  $\langle q \rangle = q_\Sigma/N$ , follows  $q_x$  in many small steps. In each lobe  $\langle q \rangle$  takes a rational value. Again we have shown this only for vanishing  $E_j$ , but in analogy to the self-charging limit, where the extension has been confirmed by quantum Monte Carlo simulations, we expect that this property does not change as long as we stay away from the phase transition. Configurations with a high commensurability have a relatively low energy and lead to particularly pronounced lobes. Therefore,  $\langle q \rangle$  is not simply equal to  $q_x$ , rather it remains

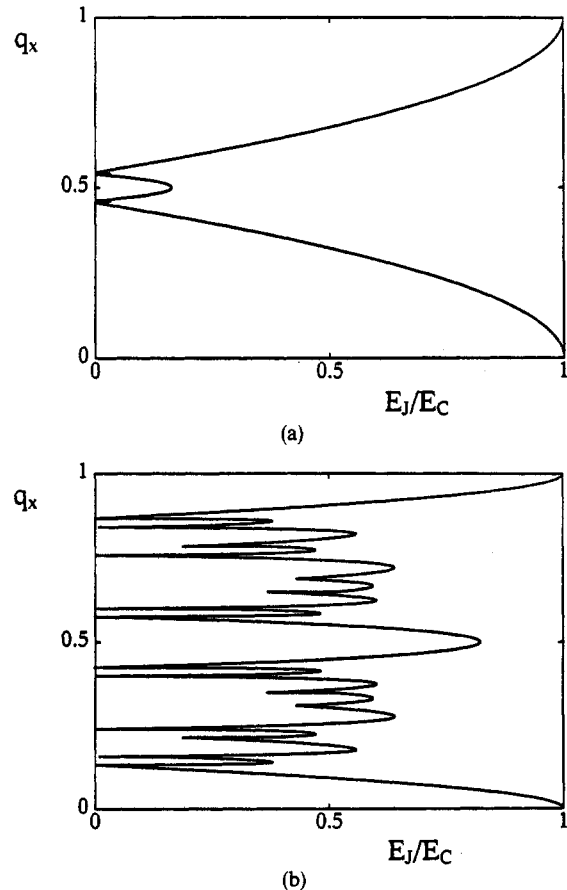


Fig. 4. Examples of phase diagrams of a  $4 \times 4$  array (with periodic boundary conditions) with a general capacitance matrix at  $T = 0$  in the presence of an external charge  $q_x$ . We have chosen (a)  $C_1 = 0.025C_0$ , (b)  $C_1 = C_0$ . The diagrams show strong commensurability effects

stuck at simple rational values (e.g. integer or half-integer) or in fact jumps already before  $q_x$  has reached such a value. In the self-charging limit we have only one big lobe and  $\langle q \rangle$  jumps from one integer to the next. In the opposite limit  $C_1 \gg C_0$  the average value  $\langle q \rangle$  is equal to  $q_x$ .

The coefficients  $\lambda$  and  $\zeta$  also show a more complicated behavior than in the self-charging case (23). The coefficient  $\lambda$  changes its sign in the center of each of the lobes shown in Fig. 4, and its dependence on  $q_x$  is not strictly linear anymore. The coefficient  $\zeta$  is constant across the lobe around  $q_x = 0$  [as given in (23)], but in general it develops structure and increases towards the edges of a given lobe.

At  $T = 0$  and  $q_x = 0$  the mean field phase boundary is given by  $E_J/E_C = 1$ . In the limit where  $C_0$  vanishes the diagonal element  $C_{00}^{-1} \propto E_C$  diverges. (For  $C_0 = 0$  it grows logarithmically with system size, in the same way as the energy of a single vortex in a junction array.) This would imply that the system remains in the disordered phase for arbitrarily large values of  $E_J$ . However, this result is an artifact of the coarse-graining approach. The duality discussed in Section 3, as well as different mean field approximations [16] give a transition to a superconducting state at a finite ratio of  $E_J/E_1$  of order 1.

#### Magnetic frustration

In the presence of a magnetic field  $f \neq 0$  we have to return to (16). The phase boundary is given by the parameters where (16) ceases to be a positive definite quadratic form. This means we have to solve an eigenvalue problem, which is equivalent to that of a Bloch electron in a magnetic field Ref. [32] This is described by Harper's equation, which in turn had been analyzed in detail by Hofstadter [43]. The largest of the eigenvalues  $E_n(f)$  of Harper's equation translates directly into a mean field phase diagram of the junction array

$$\varepsilon(T, E_J, C^{-1}, q_x) = \max \{E_n(f)\} \quad (25)$$

Examples of the resulting phase diagrams are shown in Fig. 5 for the limit where the self-capacitances dominate  $C_0 \ll C_1$ . Notice that it is trivial to include the  $q_x$ -dependence due to the separation of the  $q_x$ - and magnetic field dependence in the Ginzburg-Landau functional (16). In the opposite limit  $C_1 \gg C_0$  duality implies that the effects of magnetic frustration on the vortex-unbinding transition is the same as the effect of offset charges on the charge-unbinding transition. This means that the self dual point does not shift if  $f = q_x$ .

For suitable junction parameters, such that the system is close to the superconductor-insulator transition, the critical value of  $f$  is small. In this limit the commensurability should not play an important role (a remaining weak positional disorder in the array makes it ineffective) and we can expand in  $f$ . In this limit the Ginzburg-Landau action (16) reduces to

$$\begin{aligned} F[\psi] = & \int_0^\beta d\tau \int d^2r \left\{ \varepsilon |\psi(\mathbf{r}, \tau)|^2 \right. \\ & + \frac{1}{8E_C g(0)} |[\nabla + i2e\mathbf{A}(\mathbf{r}, \tau)]\psi(\mathbf{r}, \tau)|^2 \\ & \left. + \lambda \psi^*(\mathbf{r}, \tau) \frac{\partial}{\partial \tau} \psi(\mathbf{r}, \tau) + \zeta \left| \frac{\partial \psi(\mathbf{r}, \tau)}{\partial \tau} \right|^2 \right\}. \quad (26) \end{aligned}$$

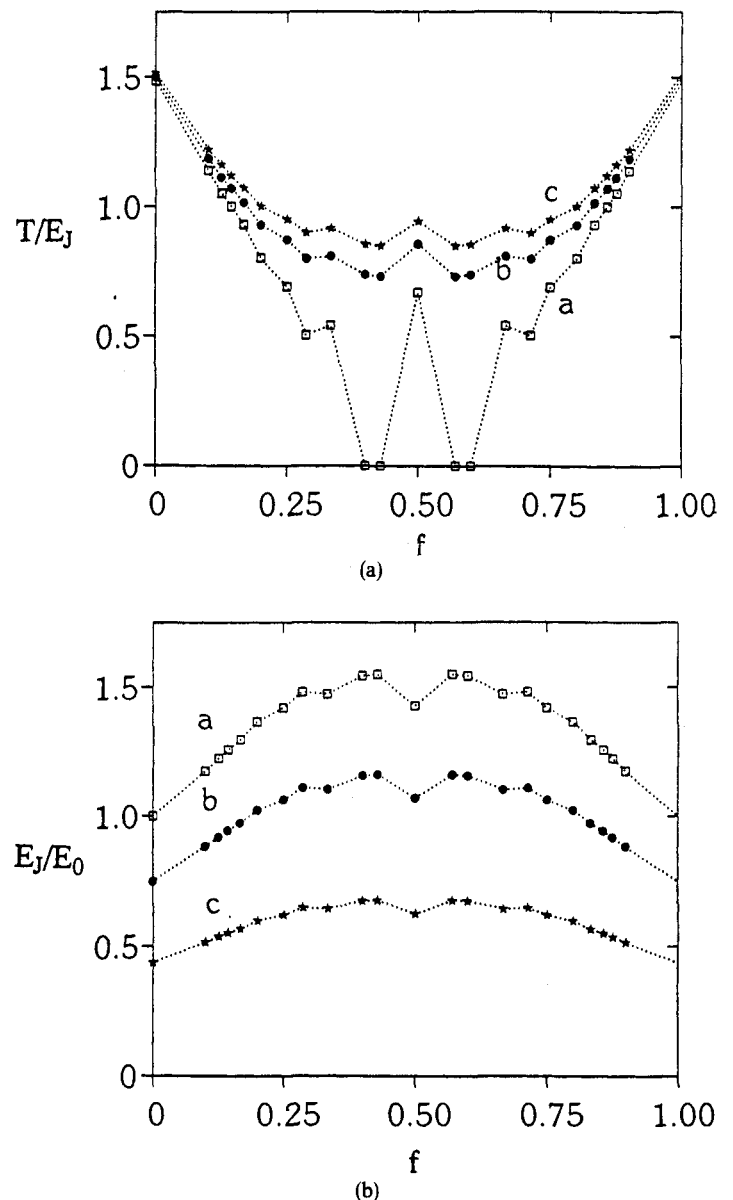


Fig. 5. Examples of phase diagrams in the presence of a magnetic field that show the typical flux periodicity and commensurability effects. (a) Phase boundary as a function of flux per plaquette  $f$  and temperature for  $E_J/E_0 = 1.5$  and  $q_x = 0$  (squares),  $\frac{1}{4}$  (dots) and  $\frac{1}{2}$  (stars). Small values of  $f$  lower the superconducting  $T_c$ . The data for  $q_x = 0$  show an interesting reentrant behavior: the region around  $f = 0.4$  remains insulating at arbitrarily low temperatures, but for  $f \approx \frac{1}{2}$ , superconductivity reappears. (b) The critical value of  $E_{J, \text{crit}}/E_0$  at  $T = 0$ . The array is superconducting above the lines for  $q_x = 0$  (squares),  $\frac{1}{4}$  (dots) and  $\frac{3}{8}$  (stars)

In the limit considered we see that the effect of a magnetic field on the properties of the junction array is precisely the same as that of a field on the properties of a superconducting film. There exists an upper critical field ( $H_{c2}$  of the film), which marks a “field-tuned” phase transition of the array as well. Its value follows from

$$\varepsilon(T, E_J, C^{-1}, q_x) + \pi f/2 = 0. \quad (27)$$

#### 5. Conductivity near the transition

##### No frustration

In the model described by (26) we can evaluate the frequency dependent conductivity explicitly. This sheds light on the properties of the disordered phase and explains the origin of the universal conductance at the transition [23]. In

order to evaluate the conductivity we study the following imaginary time correlation function

$$\sigma_{\mu\nu}(i\Omega) = \frac{1}{\Omega} \int d^2r \int_0^\beta d\tau \frac{\delta^2 \ln Z}{\delta A_\mu(\tau) \delta A_\nu(0)} e^{i\Omega\tau}, \quad (28)$$

where  $Z$  is the partition function (13). For vanishing magnetic and charge frustration the longitudinal component becomes

$$\sigma(i\Omega) = \frac{2}{R_q \beta \Omega} \int_0^\infty dk k^3 \sum_\mu G(\omega_\mu, k) \times [G(\omega_\mu, k) - G(\omega_\mu + \Omega, k)] \quad (29)$$

where

$$G(\omega_\mu, k) = \frac{1}{\zeta \omega_\mu^2 + k^2 + \varepsilon}. \quad (30)$$

In order to extract the conductivity we perform an analytic continuation to real frequencies [37]. The corresponding spectral density  $S(\omega)$  is

$$S(\omega) = \frac{\pi}{4R_q} \left(1 - \frac{4\varepsilon}{\zeta \omega^2}\right) \theta(\zeta \omega^2 - 4\varepsilon) \coth \left| \frac{\beta \omega}{4} \right|. \quad (31)$$

At zero temperature the real and imaginary part of the conductivity are

$$\begin{aligned} \text{Re } \sigma(\omega) &= \frac{\pi}{8R_q} \left(1 - \frac{4\varepsilon}{\zeta \omega^2}\right) \theta(\zeta \omega^2 - 4\varepsilon) \\ \text{Im } \sigma(\omega) &= \frac{1}{8R_q} \left\{ \left( \frac{4\varepsilon}{\zeta \omega^2} - 1 \right) \right. \\ &\quad \left. \times \ln \left| \frac{2\sqrt{\varepsilon} + \sqrt{\zeta} \omega}{2\sqrt{\varepsilon} - \sqrt{\zeta} \omega} \right| - \frac{\sqrt{\varepsilon}}{2\sqrt{\zeta} \omega} \right\}. \end{aligned} \quad (32)$$

The real part clearly exhibits an excitation gap for  $\omega < \omega_c = 2\sqrt{\varepsilon/\zeta}$ . This is consistent with the fact that no dissipation was present in the model to begin with. At low frequencies we can expand the imaginary part of the conductivity in  $\omega$ . The result is  $\sigma(\omega \ll \omega_c) = i\omega C_{\text{eff}}$ . This means the system behaves as a capacitor with effective capacitance

$$C_{\text{eff}} = \frac{\sqrt{\zeta}}{12R_q \sqrt{\varepsilon}} = \frac{C_0}{12\pi \sqrt{1 - E_J/E_0}}. \quad (33)$$

(The second part of the last equation refers to the selfcharging limit.) On the insulating side of the transition the array shows a Coulomb gap. This means no current is flowing for voltage smaller than a threshold voltage which scales with  $eC_{\text{eff}}^{-1}$ . Near the transition the effective capacitance diverges as  $\varepsilon^{-1/2}$ , and the transition to the superconducting state is marked by a Coulomb gap vanishing proportional to  $\varepsilon^{1/2}$ .

Above the gap frequency  $\omega_c$  propagating Josephson plasmon modes can be excited [37], and the real part of the conductivity is finite. The gap frequency  $\omega_c$  is proportional to  $\sqrt{\varepsilon}$ , and vanishes as the transition is approached. Right at the transition there exists no gap, and a finite dc conductance equal to

$$\sigma(\varepsilon = 0, \omega = 0) = \frac{\pi}{8R_q} \quad (34)$$

emerges. This response is the universal conductivity found by Cha *et al.* [23].

At temperatures  $T \approx \sqrt{\varepsilon/4\zeta}$  a cross-over to classical behavior occurs. For  $T \gg \sqrt{\varepsilon/4\zeta}$  we find from (31)

$$\begin{aligned} \text{Re } \sigma(\omega) &= \frac{4\pi T}{8R_q |\omega|} \left(1 - \frac{4\varepsilon}{\zeta \omega^2}\right) \theta(\zeta \omega^2 - 4\varepsilon) \\ \text{Im } \sigma(\omega) &= \frac{T}{2R_q} \left\{ \left( \frac{4\varepsilon}{\zeta \omega^2} - 1 \right) \frac{1}{\omega} \ln \left| 1 - \frac{\zeta \omega^2}{4\varepsilon} \right| - \frac{1}{\omega} \right\} \end{aligned} \quad (35)$$

The excitation gap persists, however, the effective capacitance  $C_{\text{eff}}$  now diverges as  $\varepsilon^{-1}$  near the transition. It is

$$C_{\text{eff}} = \frac{T\zeta}{16R_q \varepsilon} \quad (36)$$

### Charge frustration

Charge frustration  $q_x \neq 0$  modifies the coefficient  $\varepsilon(q_x)$ , but also leads to the appearance of a term  $i\omega_\mu \lambda$  in the Ginzburg-Landau free energy functional (18) and in the Green's function (30). When evaluating the conductivity we can perform the integration over the frequencies in eq. (29) and the analytic continuation in the same way as above. The only modification is that  $\varepsilon$  in eqs (31–33) is replaced by

$$\varepsilon_{\text{eff}}(q_x) = \varepsilon(q_x) + \frac{\lambda^2}{4\zeta}, \quad (37)$$

which does not vanish at the phase transition marked by  $\varepsilon(q_x) = 0$ . In the self-charging case the combination in eq. (37) is simply equal to  $\varepsilon_{\text{eff}}(q_x) = \varepsilon(q_x = 0)$ . Again we find that at low frequencies the response of the system is that of a capacitor, and above a threshold frequency the conductivity acquires a real part. In the case  $q_x = 0$  the effective capacitance diverges at the transition and the frequency threshold vanishes. In contrast, for nonzero  $q_x$  both remain finite up to the transition. This means the Coulomb gap vanishes in a stepwise fashion as we cross the superconducting phase transition. Furthermore, there is no indication for a universal conductivity at the transition. The nature of the phase transition differs in the system with charge frustration from that without (at the centers of the main lobes in the phase diagram) [23].

### Magnetic field effects

The effect of a magnetic field, if we neglect commensurability effects, is described by the eq. (27) (in Ref. [36] it is outlined how to treat commensurability effects in the coarse-graining approach). In this case we can take the magnetic field into account by replacing the integral over  $k$  in (29) by a sum over Landau levels  $n$ . Hence eq. (29) is replaced by

$$\begin{aligned} \sigma(i\Omega) &= \frac{(\pi f)^2}{R_q \beta \Omega} \sum_{n=0}^{\infty} \sum_{\mu} (n+1) G(\omega_\mu, n+1) \\ &\quad \times [G(\omega_\mu, n) - G(\omega_\mu + \Omega, n)] \end{aligned} \quad (38)$$

where

$$G(\omega_\mu, n) = \frac{1}{\zeta \omega_\mu^2 + \pi f n + \varepsilon_{\text{eff}}}, \quad \varepsilon_{\text{eff}}(f) = \pi f/2 + \varepsilon. \quad (39)$$

The mean field phase transition is determined by  $\varepsilon_{\text{eff}}(f) = 0$ . The real and imaginary parts of the conductivity are

$$\begin{aligned} \text{Re } \sigma(\omega) &= \frac{\pi(\pi f)^2}{\zeta^{3/2} 4R_q} \sum_{n=0}^{\infty} \frac{(n+1) \coth \frac{\beta}{2} u_{n+1}}{u_n u_{n+1} (u_n + u_{n+1})} \\ &\quad \times [\delta(\omega - u_n - u_{n+1}) + \delta(\omega + u_n + u_{n+1})] \\ \text{Im } \sigma(\omega) &= \frac{(\pi f)^2}{\zeta^2 4R_q} \sum_{n=0}^{\infty} \frac{(n+1) \coth \frac{\beta}{2} u_{n+1}}{u_n u_{n+1} (u_n + u_{n+1})} \\ &\quad \times \left( \frac{1}{u_n + u_{n+1} - \omega} - \frac{1}{u_n + u_{n+1} + \omega} \right) \end{aligned} \quad (40)$$

where  $u_n = \zeta^{-1/2} \sqrt{\pi f n + \varepsilon_{\text{eff}}}$  was introduced. As is clear from (40), the excitation gap frequency  $\omega_c$  is now given by

$$\omega_c = u_0 + u_1 = \zeta^{-1/2} (\sqrt{\varepsilon_{\text{eff}}} + \sqrt{\pi f + \varepsilon_{\text{eff}}}) \quad (41)$$

Just as for the charge frustrated case, the gap does not vanish at the transition. For small field or far from the transition, i.e.  $f \ll \varepsilon_{\text{eff}}(f)$ , the result for the conductivity (32) is essentially unchanged, except that  $\varepsilon$  is replaced by  $\varepsilon_{\text{eff}}(f)$ . For high  $f$  or close to the transition one can approximate the sum over Landau levels by the first (divergent) term. In this limit, at zero temperature the effective capacitance reduces to

$$C_{\text{eff}} \sim \frac{\sqrt{\zeta}}{2R_q \sqrt{\varepsilon_{\text{eff}}(f)}} \quad (42)$$

It still diverges at the transition. For temperatures  $T \gg u_1 = \zeta^{-1/2} \sqrt{\pi f + \varepsilon_{\text{eff}}}$  the behavior of the effective capacitance depends on the critical field  $f_{\text{cr}}$ , for a large range of parameters the effective capacitance is inversely proportional to the field, i.e.  $C_{\text{eff}} \sim f^{-1}$ .

In the absence of external charges the results (32–42) can also be obtained from the real time Ginzburg-Landau equation

$$\begin{aligned} \left( \varepsilon + \frac{1}{8E_C g(0)} |\nabla + i2e\mathcal{A}(\mathbf{r}, t)|^2 + \eta \frac{\partial}{\partial t} - \zeta \frac{\partial^2}{\partial t^2} \right) \psi(\mathbf{r}, t) \\ = \zeta(\mathbf{r}, t) \end{aligned} \quad (43)$$

that corresponds to the free energy (26). Here  $\zeta$  is a Langevin force with power spectrum  $\langle \zeta \zeta \rangle_{\omega} = \eta \omega \coth \beta \omega / 2$  and  $\eta$  is an infinitesimal dissipation. A fluctuation conductivity calculation [39], using the ordinary Kubo formula, now with the additional second time derivative added, also yields the results quoted above.

Non-Gaussian corrections will quantitatively modify the response functions. It is known that the Gaussian approximation to the universal conductance at the transition (where the fourth order term in the cumulant expansion for the Ginzburg-Landau free energy is most important) differs only 30% from Monte Carlo simulations [23]. Therefore, we expect that higher order corrections will not seriously alter our conclusions.

## 6. Bose-Hubbard model in the coarse-graining approach

In this section we discuss the Bose-Hubbard model on a  $d$ -dimensional cubic lattice in the absence of a magnetic field ( $\mathcal{A} = 0$ ), and in this section we focus on on-site

Coulomb interactions only

$$H = -\frac{1}{2} J \sum_{\langle i, j \rangle} \hat{\Phi}_i^\dagger \hat{\Phi}_j + h.c. + \frac{1}{2} V \sum_i \hat{n}_i (\hat{n}_i - 1) - \sum_i \mu \hat{n}_i \quad (44)$$

The chemical potential  $\mu \geq 0$  controls the total number of bosons  $N_b$  and the hopping term is restricted to nearest neighbor sites. At  $T = 0$  the Bose system is either insulating or superconducting. The corresponding phase diagram with respect to the model parameters  $\mu/V$  and  $J/V$  is conveniently sketched if we start from  $J = 0$  [23]. In this limit every site is occupied by an integer number of bosons. For  $n - 1 < \mu/V < n$  the boson occupation number is pinned at the integer value  $n \geq 1$  and the system has a vanishing compressibility  $\kappa = \partial N_b / \partial \mu$  due to an energy gap  $V$  for the transfer of one boson to a neighboring site. The energy gap decreases with increasing kinetic energy and vanishes at a critical value of  $J/V$  when the insulating Mott phases at commensurate fillings (the number of bosons per site is an integer) become a superconducting fluid. For non-integer fillings the system remains superfluid at all values of the repulsive Coulomb interaction [40]. Lobe-like shapes will therefore appear for the insulating phases in the  $\mu/V$  vs.  $J/V$  phase diagram [24]. The critical phenomena related to the zero temperature insulator–superconductor transition are expected to be the same as for the continuum Bose gas [44] except at the tips of the phase boundary lobes. There the transition of the lattice boson model takes place at fixed integer fillings and the critical behavior is that of an X-Y model in  $d + 1$  dimensions [37]. At finite temperatures the possibility of an intermediate phase arises which may have similar features like the so-called Bose glass which forms in the presence of diagonal disorder. It may be characterized by a nonvanishing compressibility but still a vanishing superfluid density [23, 38].

The partition function of the Bose-Hubbard model can be expressed as a coherent state path integral [45] in imaginary times  $0 < \tau < \beta = 1/k_B T$

$$Z = \int \prod_i \mathcal{D}\Phi_i^*(\tau) \mathcal{D}\Phi_i(\tau) e^{-(S_0 + S_1)} \quad (45)$$

$$S_0 = \int_0^\beta d\tau \sum_i [\Phi_i^* \partial_\tau \Phi_i - \mu \Phi_i^* \Phi_i + \frac{1}{2} V \Phi_i^* \Phi_i (\Phi_i^* \Phi_i - 1)] \quad (46)$$

$$S_1 = -\frac{J}{2} \int_0^\beta d\tau \sum_{\langle ij \rangle} (\Phi_i^* \Phi_j + c.c.) \quad (47)$$

The complex  $c$ -number fields  $\Phi_i(\tau)$  satisfy the periodic boundary condition  $\Phi_i(\beta) = \Phi_i(0)$ .

Our qualitative discussion suggested already that the phase diagram develops interesting structure for small  $J/V$ . Since the action  $S_0$  involves on-site terms only we will treat the hopping part as a perturbation and decouple it by a Hubbard-Stratonovich (HS) transformation. This is in fact opposite to what is most commonly done in many-body problems where the interaction part and not the kinetic energy is treated by approximate techniques.

Again we follow the standard steps of the “coarse-graining” procedure [37], i.e. we perform a cumulant expansion of  $e^{-S_1}$  to leading order in the auxiliary HS fields  $x_i(\tau)$ . The expectation value  $\langle x_i \rangle$  is linearly related to  $\langle \Phi_i \rangle$  and the HS fields therefore serve as an order parameter field for superconductivity. Since we are here mainly interested in the phase diagram it is sufficient to obtain the effective action to

quadratic order in the order parameter fields. Explicitly we find

$$Z \simeq Z_0 \int \prod_{\mathbf{k}} \mathcal{D}x_{\mathbf{k}}(\tau) \mathcal{D}x_{\mathbf{k}}^*(\tau) \times \exp \left[ - \int_0^\beta d\tau \sum_{\mathbf{k}} |x_{\mathbf{k}}(\tau)|^2 + \int_0^\beta d\tau \int_0^\beta d\tau' \times \sum_{\mathbf{k}} J_{\mathbf{k}} x_{\mathbf{k}}^*(\tau) x_{\mathbf{k}}(\tau') G(\tau - \tau') \right] \quad (48)$$

where we have introduced the correlation function

$$G(\tau - \tau') = \langle \Phi_{\mathbf{k}}^*(\tau) \Phi_{\mathbf{k}}(\tau') \rangle_0 = \frac{1}{Z_0} \int \prod_j \mathcal{D}\Phi_j^*(\tau) \mathcal{D}\Phi_j(\tau) \Phi_{\mathbf{k}}^*(\tau) \Phi_{\mathbf{k}}(\tau') e^{-S_0} \quad (49)$$

and  $Z_0$  is the partition function for  $J = 0$ . For a cubic lattice in  $d$  dimensions the kinetic energy dispersion is given by

$$J_{\mathbf{k}} = J \sum_{\mu=1}^d \cos(k_{\mu} a) \quad (50)$$

For the calculation of the correlation function  $G(\tau)$  with the  $\Phi^4$  action (46) we restrict the paths to Gaussian fluctuations around the saddle point  $\Phi_0$  of the action  $S_0$  which is determined by  $|\Phi_0|^2 = \frac{1}{2} + \mu/V$ . This approximate evaluation of  $G(\tau)$  is most accurate for  $\mu/V \gg 1$ , i.e. for large boson numbers when charge fluctuations on a single site are small. Introducing phase and amplitude of the boson fields by  $\Phi = (|\Phi_0| + A) e^{i\varphi}$  we consider for each site the effective (complex) quadratic action for phase and amplitude fluctuations

$$S_0^{\text{eff}} = -\frac{\beta V}{2} |\Phi_0|^4 + |\Phi_0| \int_0^\beta d\tau \times [2V |\Phi_0| A^2(\tau) + i(|\Phi_0| + 2A) \partial_{\tau} \varphi] \quad (51)$$

Since values of the phase which differ by  $2\pi$  are equivalent the path integral for  $G(\tau)$  also includes a summation over winding numbers  $\varphi(\beta) = \varphi(0) + 2\pi n$  [27] leading to

$$G(\tau - \tau') = \frac{1}{Z_0} \sum_n \int d\varphi_0 \int_{\varphi_0}^{\varphi_0 + 2\pi n} \mathcal{D}\varphi(\tau) \times \int \mathcal{D}A(\tau) \Phi^*(\tau) \Phi(\tau') e^{-S_0^{\text{eff}}} \quad (52)$$

Here we have already dropped the site index because the action  $S_0$  does not couple the boson fields at different sites. The coupling of phase and amplitude fluctuations requires the calculation of three separate contributions to the correlation function  $G(\tau)$ , i.e.

$$G(\tau) = |\Phi_0|^2 \langle e^{i[\varphi(\tau) - \varphi(0)]} \rangle_0 + |\Phi_0| \times \langle [A(\tau) + A(0)] e^{i[\varphi(\tau) - \varphi(0)]} \rangle_0 + \langle A(\tau) A(0) e^{i[\varphi(\tau) - \varphi(0)]} \rangle_0 \quad (53)$$

All three correlation functions are evaluated with the quadratic action (51). For brevity we give explicitly the result for the pure phase correlator and present the lengthy expressions for the amplitude correlation functions elsewhere [46].

$$\langle e^{i[\varphi(\tau) - \varphi(0)]} \rangle_0 = \frac{\vartheta_3(\pi[|\Phi_0|^2 + \tau/\beta], q)}{\vartheta_3(\pi|\Phi_0|^2, q)} e^{-V\tau(1 - \tau/\beta)/2} \quad (54)$$

Here  $q = \exp(-2\pi^2/\beta V)$  and  $\vartheta_3(z, q)$  is the Jacobi theta function [47] defined by

$$\vartheta_3(z, q) = 1 + 2 \sum_{n=1}^{\infty} \cos(2nz) q^{n^2} \quad (55)$$

which appears in (54) as a consequence of the winding number summation. Given  $G(\tau)$  the mean field boundary to the superconducting phase is determined from

$$0 = 1 - Jd \int_0^\beta d\tau G(\tau) \quad (56)$$

In Fig. 6 we plot the corresponding phase boundary in the  $\mu/V$  vs.  $J/V$  plane for different temperatures. For the lowest temperature we clearly recognize the two first lobes discussed above. In the zero temperature limit the superconducting phase extends down to  $J = 0$  for all integer values of  $\mu/V$ . The critical values of  $J/V$  at the tips of the lobes follow an envelope function which scales as  $\sim 1/|\Phi_0|^2$ . For  $d = 2$  and at a filling  $\langle \hat{n}_i \rangle = 1$  the coarse-graining result for the critical value is given by  $J_c/V = 0.139$  as compared to the value of  $J_c/V \approx \frac{1}{8}$  from quantum Monte Carlo (QMC) [40]. The mean field result therefore deviates quantitatively from the exact numbers by less than 10%. Also the asymmetric shape of the first lobe appears very similar to what was recently found in QMC calculations for the  $d = 1$  Bose-Hubbard chain [24].

With increasing temperature the lobe-like structures are smoothed and the phase boundary is shifted to larger critical values of  $J/V$ . At the tips of the lobes, however, the temperature dependence is nonmonotonic. This is more clearly displayed in Fig. 7, which reveals reentrant features at low temperatures. This behavior is very reminiscent of the analogous behavior found in early work on quantum phase models for Josephson junction arrays [10, 12]. The physics of this phenomenon is so far not understood. Whether it is a real property of the models or an artifact of the approx-

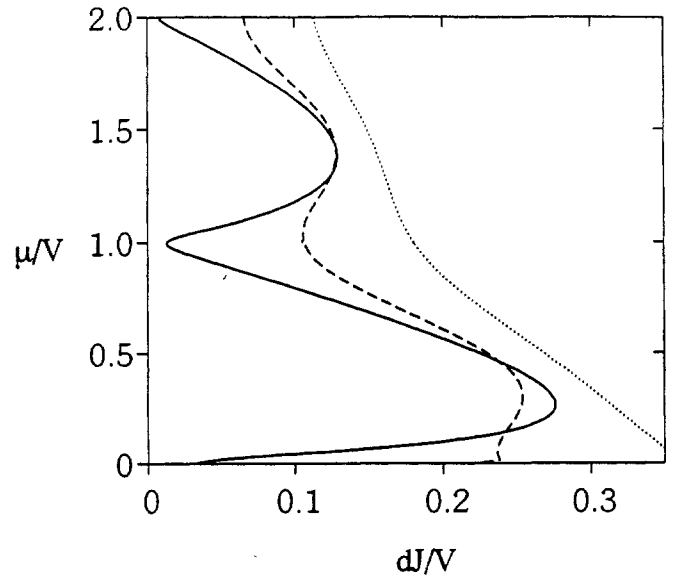


Fig. 6. "Coarse-graining" phase boundary for a  $d$ -dimensional Bose-Hubbard model at the different temperatures  $T/V = 1/100$  (solid line),  $1/10$  (dashed line), and  $1/5$  (dotted line)

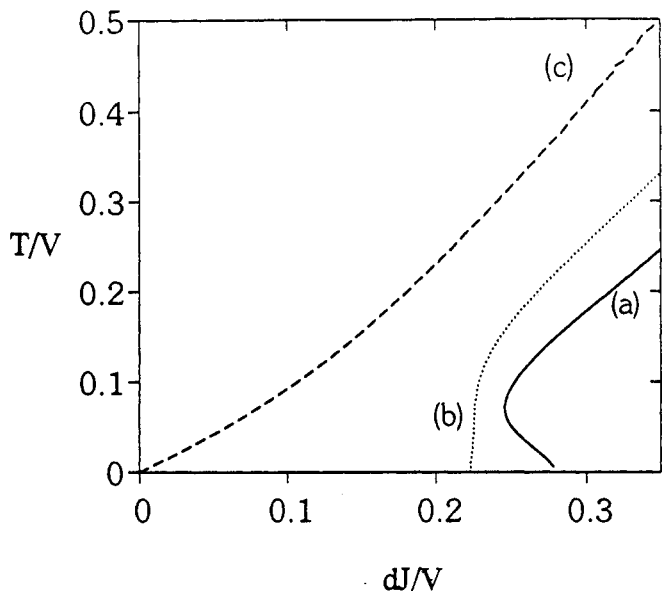


Fig. 7. Superconducting transition temperature vs.  $dJ/V$  for different values of the chemical potential. (a)  $\mu/V = \frac{1}{4}$ , (b)  $\mu/V = \frac{1}{2}$ , (c)  $\mu/V = 1$

imation schemes can be tested by the QMC techniques of Refs [24, 38, 40].

## 7. Discussion

A comparison of the phase diagrams for the Bose-Hubbard and the quantum phase model in Fig. 6 and Fig. 2, respectively, shows that the applied voltage or offset charges  $q_x = C_0 V_x/2e$  and the chemical potential  $\mu/V$  play a similar role. In both cases we find lobes of insulating phase separated by superconducting regions. For offset charges  $q_x = \pm\frac{1}{2}, \pm\frac{3}{2}, \dots$  or at integer  $\mu/V = 0, 1, \dots$  the two models lead to a superconducting state at  $T = 0$  for arbitrary strength of the Coulomb interaction. (The shift by  $\frac{1}{2}$  arises since the interaction in the Bose-Hubbard model (44) is written such that it vanishes for single site occupancy  $n_i = 1$ .)

While the phase model is perfectly periodic in  $q_x$  with period 1, there is no perfect periodicity for integer steps in  $\mu/V$  in the Bose-Hubbard model. Rather the critical coupling strength  $J/V$  for the superconductor-insulator transition at integer filling decreases inversely proportional with increasing total particle number  $N_b$ , i.e. increasing  $\mu/V$ . This shows [23] that the analogy between both models holds only for large particle numbers, if we identify  $E_j = \langle \hat{n}_i \rangle J$ .

For on-site Coulomb repulsion the phase diagram shows one insulating lobe per period, characterized by an integer occupation of the site. Finite range Coulomb repulsion leads to much more structure. Many lobes show up centered around rational values of  $q_x$ . Some of them will survive in the infinite system size limit. We modeled the finite range interaction by allowing for self-capacitance as well as nearest neighbor capacitance in the quantum phase model. It is obvious that the Bose-Hubbard model with an equivalent generalization, analyzed within the coarse-graining approach, will develop the equivalent structure. It would be interesting to verify – for instance by the quantum Monte Carlo techniques of Refs [24, 38, 40] – whether this structure is a real property of the models or an artifact of the approximation schemes.

The analysis of the conductivity, in the coarse-graining approach, is very transparent. Of course the explicit results

reveal the mean field approximation used, but we believe that several of the conclusions are valid in general. The Coulomb blockade, which has been found in many small capacitance junction systems, is responsible for the insulating behavior. The Coulomb gap vanishes at the transition. The nature of the phase transition and the response function differ in the presence or absence of charge frustration. Only for integer  $q_x$  does the threshold frequency for the real part of the conductance vanish at the transition, leading to a universal value of the conductivity.

In principle the effect of charge frustration can be checked in an array of Josephson junctions by controlling the external voltage relative to a ground plane. However, the detailed predictions for the phase diagram presented here depend essentially on the assumption that the array has no disorder. The fluctuations of the junction parameters are probably small enough to make this possible. But random offset charges due to charged impurities (which are equivalent to random on-site energies in the Bose Hubbard model) are hard to avoid. Only if their effect is weak can we expect to observe the rich structure in the phase diagram.

## Acknowledgement

We would like to acknowledge many stimulating discussions with U. Eckern, J. E. Mooij, H. van der Zant and G. Zimanyi. The work is part of the ‘‘Sonderforschungsbereich 195’’ which is supported by the ‘‘Deutsche Forschungsgemeinschaft’’. One of us (R.F.) acknowledges the support by the Heraeus Stiftung during his stay at the University of Karlsruhe.

## Appendix A. The correlation function $g_{ij}(\omega_\mu)$

According to the definition given in (17) for the correlation function, we have to calculate

$$g_{i0}(\tau) = \frac{1}{Z_0} \sum_{\{n_j\}} \prod_j \int d\varphi_{j0} \int_{\varphi_{j0}}^{\varphi_{j0} + 2\pi n_j} \mathcal{D}\varphi_f(\tau) \exp \left\{ -S_0[\varphi] + 2\pi i \sum_j q_{xj} n_j + i[\varphi_i(\tau) - \varphi_0(0)] \right\} \quad (57)$$

The partition function  $Z_0$  is expressed in a similar fashion. Using  $S_0$  given in (15) and the parametrization  $\varphi_f(\tau) = \varphi_{i0} + 2\pi i n_i \tau/\beta + \theta_f(\tau)$  we find that all the off-diagonal elements of the correlation function, viz.  $g_{i0}(\tau)$  for  $i \neq 0$  vanish because of the integrations over  $\varphi_{j0}$ . The reason is that  $S_0$  does not depend on the phase  $\varphi_f(\tau)$  itself but only on its time derivative.

It is therefore sufficient to calculate the on-site correlation function at site 0

$$g(\tau) \equiv g_{00}(\tau) = \frac{1}{Z_0} \sum_{\{n_j\}} \exp \left( 2\pi i \sum_j q_{xj} n_j - T \sum_{ij} \frac{4\pi^2}{8e^2} n_i C_{ij} n_j \right) \times \exp(-2\pi i T n_0 \tau) g_c(\tau) \quad (58)$$

where  $g_c(\tau)$ , the correlation function for the case of continuous charges, results from the remaining integral over  $\theta(\tau)$ . It is [48]

$$g_c(\tau) = \exp[-2e^2 C_{00}^{-1} \tau(1 - \tau T)] \quad (59)$$

and

$$C_{00}^{-1} = \frac{1}{N} \sum_k \frac{1}{C(k)}. \quad (60)$$

The Poisson resummation formula

$$\sum_{\{n_i\}} \exp \left( - \sum_{ij} n_i A_{ij} n_j + 2 \sum_i z_i n_i \right) \\ = \sqrt{\frac{\pi^N}{\det A}} \sum_{\{q_i\}} \exp \left[ - \sum_{ij} (\pi q_i + z_i) A_{ij}^{-1} (\pi q_j + z_j) \right] \quad (61)$$

plus a subsequent Fourier transform  $g(\omega_\nu) = \int_0^\beta \exp(i\omega_\nu \tau) g(\tau) d\tau$  lead to

$$g(\omega_\nu) = \frac{1}{Z_0} \sum_{\{q_i\}} \exp \left[ - \frac{2e^2}{T} \sum_{ij} (q_i - q_x) C_{ij}^{-1} (q_j - q_x) \right] \\ \times \frac{4e^2 C_{00}^{-1}}{[2e^2 C_{00}^{-1}]^2 - \left[ 4e^2 \sum_j C_{0j}^{-1} (q_j - q_x) - i\omega_\nu \right]^2} \quad (62)$$

from which expression (22) follows.

## References

1. For a number of articles see the Proceedings of the NATO Advanced Research Workshop on Coherence in Superconducting Networks, (Edited by J. E. Mooij and G. Schön), *Physica Scripta* **B152**, (1988).
2. Kosterlitz, J. M. and Thouless, D. J., *J. Phys. C* **6**, 1181, (1973); Berezinskii, V. L., *Zh. Eksp. Teor. Fiz.* **59**, 907 (1970) [*Sov. Phys. JETP*, **32**, 493 (1971)].
3. Teitel, S. and Yayaaprakash, C., *Phys. Rev.* **B27**, 598 (1983); Shih, W. Y. and Stroud, D., *Phys. Rev.* **B28**, 6575 (1983); Choi, M. Y. and Doniach, S., *Phys. Rev.* **B31**, 4516 (1985); Halsey, T. C., in Ref. [1]; Minnhagen, P. and Weber, H., in Ref. [1]; van Himbergen, J. E., in Ref. [1].
4. Anderson, P. W., in "Lectures on the Many-Body Problem" (Edited by E. R. Caianello), Vol. 2, 113, (Academic 1964); Abeles, B., *Appl. Sol. State Science* **6**, 1 (1975).
5. A large number of articles dealt with this problem. We quote here only two: Jacobs, L., Jose, J. V. and Novotny, M. A., *Phys. Rev. Lett.* **51**, 2177 (1984); Simanek, E., *Solid State Comm.* **31**, 419 (1979).
6. Chakravarty, S. *et al.*, *Phys. Rev. Lett.* **56**, 2303 (1986); Kampf, A. and Schön, G., *Phys. Rev.* **B36**, 3651 (1987); Fisher, M. P. A., *Phys. Rev.* **B36**, 1917 (1987); Zwerger, W., *J. Low Temp. Phys.* **72**, 291 (1988); Fazio, R., Falci, G. and Giaquinta, G., *Solid State Comm.* **71**, 275 (1989); for further references see also [1].
7. Orr, B. G., Jaeger, H. M., Goldman, A. M. and Kuper, C. G., *Phys. Rev. Lett.* **56**, 378 (1986) Jaeger, H. M., Haviland, D. B., Liu Y. and Goldman, A. M., *Phys. Rev.* **B40**, 182 (1989); Haviland, D. B., Orr, B. G. and Goldman, A. M., *Phys. Rev.* **B40**, 182 (1989); Haviland, D. B., Liu, Y. and Goldman, A. M., *Phys. Rev. Lett.* **62**, 2180 (1989).
8. Geerligs, L. J., Peters, M., de Groot, L. E. M., Verbruggen, A. and Mooij, J. E., *Phys. Rev. Lett.* **63**, 326 (1989).
9. Chen, C. and Delsing, P., *Helvetica Physica Acta*, Proceedings of the Conference "Physics in 2 Dimensions", (to be published); Delsing, P., Chen, C. and Claeson, T., in "SQUID'91, Springer Proceedings in Physics" (Edited by H. Koch), (to be published).
10. Efetov, K. B., *Sov. Phys. JETP* **51**, 1015 (1980).
11. Bradley, R. M. and Doniach, S., *Phys. Rev.* **B30**, 1138 (1984).
12. Fazekas, P., Mühlischlegel, B. and Schröter, M., *Z. Phys.* **B57**, 193 (1984).
13. Fisher, M. P. A., *Phys. Rev.* **B36**, 1917 (1987).
14. Fishman, R. S. and Stroud, D., *Phys. Rev.* **B38**, 290 (1988).
15. Mirhashem, B. and Ferrell, R. A., *Phys. Rev.* **B37**, 649 (1988).
16. The result of the analysis of J. Kissner (unpublished) is presented by Eckern, U. and Schön, G., in "Festkörperprobleme", *Advances in Solid State Physics* **29**, (Vieweg 1989), 1.
17. Mooij, J. E., van Wees, B. J., Geerligs, L. J., Peters, M., Fazio, R. and Schön, G., *Phys. Rev. Lett.* **65**, 645 (1990).
18. Mooij, J. E. and Schön, G., in "Single Charge Tunneling" (Edited by H. Grabert and M. Devoret) (NATO ASI Series, Les Houches 1991), (to be published).
19. Fazio, R. and Schön, G., *Phys. Rev.* **B43**, 5307 (1991); and in "Transport Properties of Superconductors - Progress in High  $T_c$ " (Edited by R. Nikolsky), (World Scientific 1990), vol. **25**, p. 298.
20. Sugahara, M. and Yoshikawa, N., "Extended Abstracts of the 1987 International Superconductivity Electronics Conference (1987)", p. 341; Yoshikawa, N., Akeyoshi, T., Kojima, M. and Sugahara, M., *Jpn. J. Appl. Phys.* **26**, 949 (1987).
21. van Wees, B. J., *Phys. Rev.* **B44**, 2264 (1991).
22. Fazio, R., van Otterlo, A., Schön, G., van der Zant, H. S. J. and Mooij, J. E., Proceedings of the Conference "Physics in 2 Dimensions", *Helvetica Physica Acta*, (to be published).
23. Fisher, M. P. A., Grinstein, G. and Girvin, S. M., *Phys. Rev. Lett.* **64**, 587 (1990); Fisher, M. P. A., Weichman, B. P., Grinstein, G. and Fisher, D. S., *Phys. Rev.* **B40**, 546 (1989); Cha, M.-C., Fisher, M. P. A., Girvin, S. M., Wallin, M. and Young, A. P., *Phys. Rev.* **B44**, 6883 (1991).
24. Batrouni, G. G., Scalettar, R. T. and Zimanyi, G. T., *Phys. Rev. Lett.* **65**, 1765 (1990).
25. Niyaz, P., Scalettar, R. T., Fong, C. Y. and Batrouni, G. G., *Phys. Rev.* **B44**, 7143 (1991).
26. Feigel'man, M. V. and Ziegler, K. (unpublished).
27. Schön, G. and Zaikin, A. D., *Phys. Rep.* **198**, 237 (1990).
28. Fazio, R., Geigenmüller, U. and Schön, G., in "Quantum Fluctuations in Mesoscopic and Macroscopic Systems" (Edited by H. A. Cerdeira *et al.*), (World Scientific 1991), p. 214.
29. Chakravarty, S., Kivelson, S., Zimanyi, G. T. and Halperin, B. I., *Phys. Rev.* **B35**, 7356 (1987).
30. Korshunov, S. E., *Europhys. Lett.* **9**, 107 (1989); Zwerger, W., *Europhys. Lett.* **9**, 421 (1989).
31. Bobbert, P. A., Fazio, R., Schön, G. and Zimanyi, G. T., *Phys. Rev.* **B41**, 4009 (1990); Bobbert, P. A., Fazio, R., Schön, G. and Zaikin, A. D., *Phys. Rev.* **B45**, 2294 (1992).
32. Kampf, A. and Schön, G., *Phys. Rev.* **B37**, 5954 (1988).
33. Fisher, M. P. A., *Phys. Rev. Lett.* **65**, 923 (1990).
34. Hebard, A. F. and Paalanen, M. A., *Phys. Rev. Lett.* **65**, 927 (1990).
35. van der Zant, H. S. J., Fritschy, F. C., Eliou, W. E., Geerligs, L. J. and Mooij, J. E., submitted to *Phys. Rev. Lett.*
36. Granato, E. and Kosterlitz, J. M., *Phys. Rev. Lett.* **65**, 1267 (1990).
37. Doniach, S., *Phys. Rev.* **B24**, 5063 (1981); in "Percolation, Localization and Superconductivity", Proceedings of the NATO Advanced Research Workshop, (Edited by A. M. Goldman and S. A. Wolf) (Plenum, 1984).
38. Scalettar, R. T., Batrouni, G. G. and Zimanyi, G. T., *Phys. Rev. Lett.* **66**, 3144 (1991).
39. See for instance Tilley, D. R. and Parkinson, J. B., *J. Phys.* **C2**, 2175 (1969).
40. Krauth, W. and Trivedi, N., *Europhys. Lett.* **14**, 627 (1991).
41. Fisher, M. P. A., *Physica Scripta* **A177**, 553 (1991).
42. Caldeira, A. O. and Leggett, A. J., *Phys. Rev. Lett.* **46**, 211 (1981).
43. Hofstadter, D. R., *Phys. Rev.* **B14**, 2239 (1976).
44. Weichman, P. B., *Phys. Rev.* **B38**, 8739 (1988).
45. See e.g. Schulman, L. S., "Techniques and Applications of Path Integration" (John Wiley, New York 1981), Chapter 27.
46. Kampf, A. P., (unpublished).
47. Whittaker, E. T. and Watson, G. N., "A Course of Modern Analysis" (Cambridge University Press 1962).
48. Simanek, E., *Phys. Rev.* **B32**, 500 (1985).